

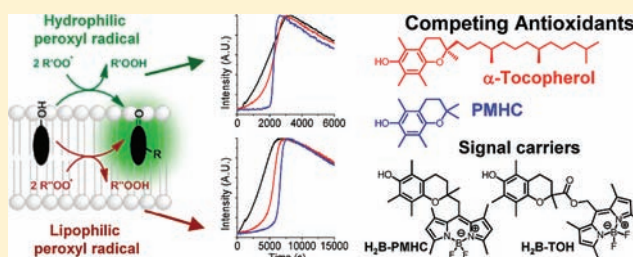
# How Lipid Unsaturation, Peroxyl Radical Partitioning, and Chromanol Lipophilic Tail Affect the Antioxidant Activity of $\alpha$ -Tocopherol: Direct Visualization via High-Throughput Fluorescence Studies Conducted with Fluorogenic $\alpha$ -Tocopherol Analogues

Katerina Krumova, Sayuri Friedland, and Gonzalo Cosa\*

Department of Chemistry and Center for Self Assembled Chemical Structures, McGill University, 801 Sherbrooke Street West, Montreal, Quebec H3A 2K6, Canada

**S** Supporting Information

**ABSTRACT:** The preparation of two highly sensitive fluorogenic  $\alpha$ -tocopherol (TOH) analogues which undergo >30-fold fluorescence intensity enhancement upon reaction with peroxy radicals is reported. The probes consist of a chromanol moiety coupled to the *meso* position of a BODIPY fluorophore, where the use of a methylene linker (BODIPY-2,2,5,7,8-pentamethyl-6-hydroxy-chroman adduct, H<sub>2</sub>B-PMHC) vs an ester linker (*meso*-methanoyl BODIPY-6-hydroxy-2,5,7,8-tetramethylchromane-2-carboxylic acid, H<sub>2</sub>B-TOH) enables tuning their reactivity toward H-atom abstraction by peroxy radicals. The development of a high-throughput fluorescence assay for monitoring kinetics of peroxy radical reactions in liposomes is subsequently described where the evolution of the fluorescence intensity over time provides a rapid, facile method to conduct competitive kinetic studies in the presence of TOH and its analogues. A quantitative treatment is formulated for the temporal evolution of the intensity in terms of relative rate constants of H-atom abstraction ( $k_{inh}$ ) from the various tocopherol analogues. Combined, the new probes, the fluorescence assay, and the data analysis provide a new method to obtain, in a rapid, parallel format, relative antioxidant activities in phospholipid membranes. The method is exemplified with four chromanol-based antioxidant compounds differing in their aliphatic tails (TOH, PMHC, H<sub>2</sub>B-PMHC, and H<sub>2</sub>B-TOH). Studies were conducted in six different liposome solutions prepared from poly- and mono-unsaturated and saturated (fluid vs gel phase) lipids in the presence of either hydrophilic or lipophilic peroxy radicals. A number of key insights into the chemistry of the TOH antioxidants in lipid membranes are provided: (1) The relative antioxidant activities of chromanols in homogeneous solution, arising from their inherent chemical reactivity, readily translate to the microheterogeneous environment at the water/lipid interface; thus similar values for  $k_{inh}^{H_2B-PMHC}/k_{inh}^{H_2B-TOH}$  in the range of 2–3 are recorded both in homogeneous solution and in liposome suspensions with hydrophilic or lipophilic peroxy radicals. (2) The relative antioxidant activity between tocopherol analogues with the same inherent chemical reactivity but bearing short (PMHC) or long (TOH) aliphatic tails,  $k_{inh}^{PMHC}/k_{inh}^{TOH}$ , is  $\sim 8$  in the presence of hydrophilic peroxy radicals, regardless of the nature of the lipid membrane into which they are embedded. (3) Antioxidants embedded in saturated lipids do not efficiently scavenge hydrophilic peroxy radicals; under these conditions wastage reactions among peroxy radicals become important, and this translates into larger times for antioxidant consumption. (4) Lipophilic peroxy radicals show reduced discrimination between antioxidants bearing long and short aliphatic tails, with  $k_{inh}^{PMHC}/k_{inh}^{TOH}$  in the range of 3–4 for most lipid membranes. (5) Lipophilic peroxy radicals are scavenged with the same efficiency by all four antioxidants studied, regardless of the nature of their aliphatic tail or the lipid membrane into which they are embedded. These data underpin the key role the lipid environment plays in modulating the rate of reaction of antioxidants characterized by similar inherent chemical reactivity (arising from a conserved chromanol moiety) but differing in their membrane mobility (structural differences in the lipophilic tail). Altogether, a novel, facile method of study, new insights, and a quantitative understanding on the critical role of lipid diversity in modulating antioxidant activity in the lipid milieu are reported.



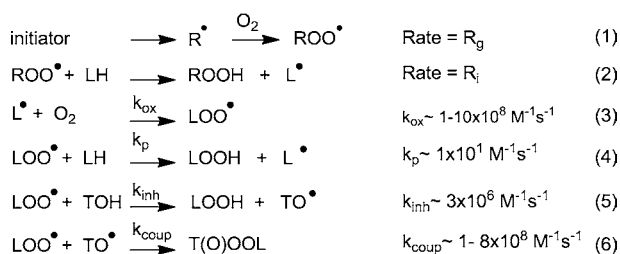
## INTRODUCTION

A member of the vitamin E family of compounds,  $\alpha$ -tocopherol (TOH) has long been recognized as the most active naturally occurring, lipid-soluble antioxidant (Scheme 1 and Figure 1, below).<sup>1</sup> Interest in the antioxidant and anti-inflammatory properties of TOH has led to multiple studies proposing among others the benefit of TOH in mitigating cardiovascular disease,<sup>2</sup>

slowing Alzheimer's disease progression,<sup>3</sup> and most recently promoting plasma membrane repair.<sup>4</sup> TOH has also attracted attention due to its non-antioxidant functions, in particular its emerging role as a cellular signaling molecule, including

Received: February 20, 2012

Published: May 8, 2012

**Scheme 1. Lipid Oxidation in the Presence of a Free Radical Initiator (ROO•) and TOH<sup>a,9</sup>**


<sup>a</sup>Here LH represents a bis-allylic methylene moiety. The listed rate constants were obtained in homogeneous solutions. Equation 3, ref 7; eq 4, ref 8; eq 5, ref 1; eq 6, ref 9.

modulation of the activity of protein kinase C<sup>5</sup> and phosphatidylinositol 3-kinase as well as regulation of a number of genes.<sup>6</sup>

In a first elementary step, TOH reacts with a peroxy radical (ROO• or LOO•) via H-atom transfer to yield a tocopheroxyl radical (TO•, eq 5) and a hydroperoxide (ROOH/LOOH). Analysis of the rate law for the overall process shows that the antioxidant activity of TOH is given by the rate constant for this second-order reaction ( $k_{\text{inh}}$ , the rate constant of H-atom abstraction). In the next elementary step, the TO• initially formed rapidly scavenges a second ROO•/LOO• to yield addition products (e.g., tocopherones, eq 6).<sup>1,10–12</sup> In the presence of initiators and in homogeneous solution, TOH thus scavenges two peroxy radicals. The rate of generation  $R_g$  of peroxy radicals may be equal to the rate of initiation  $R_i$  of lipid peroxidation and is calculated by measuring the rate of consumption of TOH,<sup>1</sup>

$$-\frac{d[\text{TOH}]}{dt} = k_{\text{inh}}^{\text{TOH}}[\text{LOO}^\bullet][\text{TOH}] = \frac{R_g}{2} \quad (7)$$

Whereas the antioxidant activities of TOH, its analogues,<sup>13</sup> and other natural and synthetic lipophilic phenolic compounds including catechols,<sup>14</sup> dihydroquinones,<sup>15–17</sup> naphthyridinols,<sup>18</sup> etc. are well established in homogeneous solution in organic solvents, their quantification in model lipid membranes is significantly more difficult. Structural and stereoelectronic effects account for TOH's rapid H-atom transfer to peroxy free radicals in homogeneous solution.<sup>1</sup> When TOH is embedded in lipid membranes, in addition to its inherent chemical reactivity, both its localization/accessibility and its mobility in heterogeneous media play roles in modulating its relative rate of free radical scavenging.<sup>8,10,19–31</sup> In line with the above, a ~1000-fold reduction in  $k_{\text{inh}}$  has been reported for TOH in phospholipid membranes vs in organic solution,<sup>20</sup> mostly attributed to TOH's physical inaccessibility to attacking radicals and only minimally due to hydrogen-bonding to water (hydrogen atom transfer cannot take place between a phenol antioxidant (AOH) when it is hydrogen-bonded to the solvent, for steric reasons<sup>32–34</sup>). In fact, estimates of the drop in  $k_{\text{inh}}$  for TOH based solely on the interaction with water place the value at  $8 \times 10^5 \text{ M}^{-1} \text{ s}^{-1}$ , only 4-fold smaller than the  $3 \times 10^6 \text{ M}^{-1} \text{ s}^{-1}$  value reported in styrene.<sup>19</sup>

The strong effect imparted on  $k_{\text{inh}}$  by the physical-chemical heterogeneity of the phospholipid membrane/water interface is highlighted by the different antioxidant activities measured for 2,2,5,7,8-pentamethyl-6-hydroxy-chroman (PMHC, a TOH analogue lacking the phytol tail) and TOH (see Figure 1 for

their chemical structures), a topic which was recently reviewed.<sup>8</sup> Both molecules have the same inherent chemical reactivity toward peroxy radicals, arising from the conserved chromanol moiety, yet within phospholipid membranes and due to its higher mobility, PMHC is a more potent antioxidant than TOH.<sup>8</sup> While a significant body of research has been dedicated to the role of the media in determining antioxidant activities, how the rich diversity in the lipid membrane composition affects the mobility and consequently the relative antioxidant activity of TOH is still poorly understood.<sup>35–39</sup>

In order to provide a quantitative understanding of the role that the lipid environment plays in the relative antioxidant activities of TOH and its analogues, we have developed a fluorescence-based method to study the relative antioxidant activities of TOH and its analogues in a rapid, parallel format. The method relies on three key elements: (1) The preparation of two new, highly sensitive fluorogenic TOH analogues that follow conceptually the design of the first-generation probe B-TOH that we recently reported,<sup>40,41</sup> yet they have a much higher sensitivity. The new probes reported here undergo >30-fold fluorescence intensity enhancements upon reaction with peroxy radicals. Their reactivity toward peroxy radicals was further tuned to provide suitable references for competitive kinetic studies using the probes as signal carriers. (2) A simple high-throughput fluorescence assay for a microplate reader that relies on the high sensitivity of the two new probes and that reports real-time ROO• reaction dynamics with TOH and its analogues in compartmented systems. (3) A quantitative treatment of the temporal evolution of the fluorescence intensity wherefrom the kinetic information is obtained for the various conditions analyzed.

With this new method, we show here how the membrane fluidity (gel vs liquid-crystalline phase) and extent of lipid unsaturation, the type of peroxy radical used (lipophilic vs hydrophilic), and the lipophilic tail in the free radical scavenger all affect the relative antioxidant dynamics of TOH and its analogues. Quantitative results validate the robustness of the new method described. Most importantly, they provide a wealth of information and new insights on the critical role of lipid diversity in modulating antioxidant activity in the lipid milieu.

## RESULTS AND DISCUSSION

**Preparation of the New Probes.** The two new fluorogenic antioxidants synthesized for our studies are shown in Figure 1. The two-segment receptor–reporter probes consist of a chromanol moiety coupled to the *meso* position of a BODIPY fluorophore, either via an ester linker (*meso*-methanoyl BODIPY-6-hydroxy-2,5,7,8-tetramethylchromane-2-carboxylic acid, H<sub>2</sub>B-TOH) or via a methylene linker

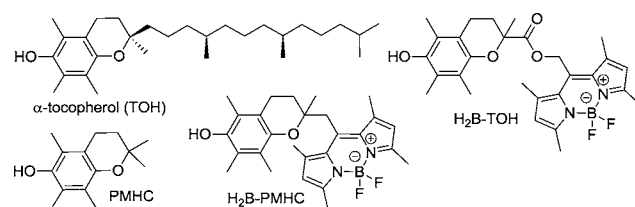


**Figure 1.** Structures of TOH, PMHC, and the new probes H<sub>2</sub>B-TOH and H<sub>2</sub>B-PMHC.

(BODIPY-2,2,5,7,8-pentamethyl-6-hydroxy-chroman adduct, or H<sub>2</sub>B-PMHC).

The new fluorogenic antioxidants follow the conceptual design of the first-generation probe B-TOH that we recently reported.<sup>40,41</sup> They rely on an intramolecular off–on switch based on photoinduced electron transfer<sup>42</sup> from the chromanol to the BODIPY moiety. The chromanol moiety quenches the emission of the fluorophore until it is oxidized following reaction with peroxy radicals.<sup>40,41,43</sup> A BODIPY dye with improved redox potential recently prepared by us<sup>44</sup> was utilized as the reporter segment in both H<sub>2</sub>B-TOH and H<sub>2</sub>B-PMHC. Favorable photoinduced electron transfer from the chromanol to the BODIPY group ensures an excellent contrast between the dark (reduced) and emissive (oxidized) states, which is required for the high-throughput fluorescence method described here.

H<sub>2</sub>B-TOH was prepared by coupling 6-hydroxy-2,5,7,8-tetramethylchromane-2-carboxylic acid, commercially known as Trolox (Hoffman-LaRoche), to the BODIPY dye 8-hydroxymethyl-1,3,5,7-tetramethyl pyrromethene fluoroborate via a new route involving Mitsunobu reaction. This methodology gave the product with much better yields than the coupling we originally reported in preparing B-TOH, involving EDC.<sup>41</sup> The new compound was prepared with a 67% yield. H<sub>2</sub>B-TOH undergoes ~30-fold intensity enhancement upon scavenging peroxy radicals when embedded in lipid membranes, a marked improvement over the 4-fold enhancement<sup>43</sup> originally reported for B-TOH under similar conditions.

The rationale behind the preparation of H<sub>2</sub>B-PMHC was to tune the rate constants of H-atom abstraction ( $k_{inh}$ ) or antioxidant activity of the probe by utilizing a methylene rather than an ester linker to couple the BODIPY dye to the chromanol moiety. It has been found experimentally that TOH has a larger  $k_{inh}$  value than Trolox:  $k_{inh} = 3.2 \times 10^6$  and  $1.1 \times 10^6 \text{ M}^{-1} \text{ s}^{-1}$ , respectively, in styrene.<sup>13</sup> The smaller value recorded for Trolox is due to the electron-withdrawing effect of the carboxylic moiety, which strengthens the phenol O–H bond.<sup>13</sup> We reasoned that, by replacing the carbonyl linker by a methylene linker in our probes, we would achieve a similar difference in reactivity between H<sub>2</sub>B-TOH and H<sub>2</sub>B-PMHC (Scheme 2).

Key in designing H<sub>2</sub>B-PMHC was also to minimize the distance between the receptor and reporter segments to ensure

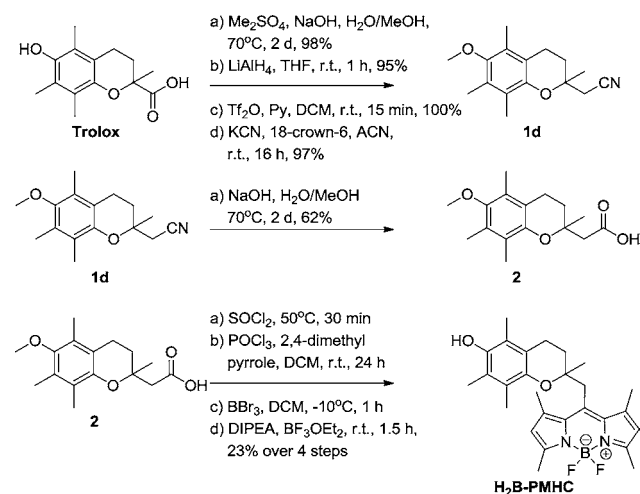
that efficient photoinduced electron transfer takes place from the chromanol to the BODIPY segment, ensuring a dark “off” state and better overall sensitivity for the off–on probe. We thus initially considered preparing the probe by building the BODIPY dye directly onto the acid chloride derivative of Trolox. We were, however, unsuccessful in our attempts, presumably due to the steric crowding around the quaternary carbon in the chromanol ring. We thus extended the aliphatic chain in Trolox by first reducing the acid group to an alcohol, followed by the insertion of a good leaving group (triflate), substitution by nitrile (**1d** in Scheme 2), and hydrolysis to obtain the desired acid, 2-(6-methoxy-2,5,7,8-tetramethylchroman-2-yl)-acetic acid (**2** in Scheme 2). The acid chloride was next prepared, and it was reacted with 2 equiv of 2,4-dimethylpyrrole in the presence of phosphorus oxychloride. The organic compound was subsequently deprotected with BBr<sub>3</sub>, and following addition of DIPEA and BF<sub>3</sub>·OEt<sub>2</sub>, we obtained H<sub>2</sub>B-PMHC in 23% yield from **2**.

**Fluorescence Assay.** The two new probes were used as signal carriers in competitive kinetic studies in the presence of TOH and PMHC. These studies yielded relative antioxidant activity values in model lipid membranes for either TOH or PMHC vs either H<sub>2</sub>B-TOH or H<sub>2</sub>B-PMHC. In our assay, we used a microplate reader to monitor over time the emission intensity enhancement of membrane-embedded H<sub>2</sub>B-TOH or H<sub>2</sub>B-PMHC upon scavenging peroxy radicals when alone or in the presence of competing antioxidants.

We conducted our experiments with liposomes prepared from six different glycerophospholipids chosen on the basis of both the degree of unsaturation in their fatty acid chains and their transition temperature ( $T_m$ ). We prepared aqueous dispersions of liposomes of L- $\alpha$ -phosphocholine (eggPC, a natural mixture containing saturated, unsaturated, and polyunsaturated fatty acids, mostly 16:0 and 18:1-*cis*-9), 1,2-dilinoleoyl-*sn*-glycero-3-phosphocholine (DLPC, 18:2-*cis*-9, *cis*-12 polyunsaturated fatty acids,  $T_m = -53 \text{ }^\circ\text{C}$ ), 1,2-dioleoyl-*sn*-glycero-3-phosphocholine (DOPC, 18:1-*cis*-9 unsaturated fatty acids,  $T_m = -20 \text{ }^\circ\text{C}$ ), 1-palmitoyl-2-oleoyl-*sn*-glycero-3-phosphocholine (POPC, 16:0 saturated and 18:1-*cis*-9 unsaturated fatty acid,  $T_m = -2 \text{ }^\circ\text{C}$ ), 1,2-dimyristoyl-*sn*-glycero-3-phosphocholine (DMPC, 14:0 saturated fatty acids,  $T_m = 23 \text{ }^\circ\text{C}$ ), and 1,2-dipalmitoyl-*sn*-glycero-3-phosphocholine (DPPC, 16:0 saturated fatty acids,  $T_m = 41 \text{ }^\circ\text{C}$ ). The liposome dispersions were prepared following standard protocols involving the hydration and subsequent extrusion of lipid films through 100 nm polycarbonate films.<sup>45</sup> The pH 6.7, 10 mM phosphate-buffered saline (PBS) solutions were 150 mM in NaCl and  $1 \times 10^{-3} \text{ M}$  in lipid ( $\sim 1 \times 10^{-8} \text{ M}$  in liposomes).<sup>45</sup>

Liposome dispersions were supplemented with acetonitrile solutions containing increasing concentrations of H<sub>2</sub>B-TOH (or H<sub>2</sub>B-PMHC) ranging from  $8.5 \times 10^{-7}$  to  $6.1 \times 10^{-6} \text{ M}$ . Alternatively, in competing kinetic studies, a constant concentration of H<sub>2</sub>B-TOH (or H<sub>2</sub>B-PMHC) of  $1 \times 10^{-7} \text{ M}$  was used with either PMHC or TOH at concentrations ranging from  $7.5 \times 10^{-7}$  to  $6 \times 10^{-6} \text{ M}$ . The lipid:antioxidant ([LH]:[AOH]) mole ratio in our experiments extended from  $1 \times 10^4$  to  $1.7 \times 10^2$ , within the range of values encountered in the membranes of many cells,<sup>35,36,46</sup> and below the critical value for [LH]:[AOH] =  $1 \times 10^5$ , above which lipid peroxidation via a chain reaction will be observed for polyunsaturated fatty acids (PUFAs).<sup>23</sup> Under our experimental conditions in the presence of an antioxidant, the kinetic chain length for PUFA lipid

**Scheme 2. Preparation of H<sub>2</sub>B-PMHC**



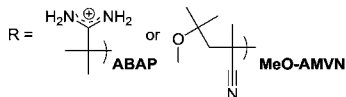
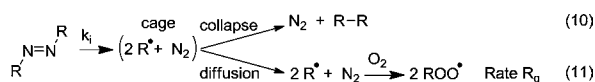
autoxidation  $\nu$  is negligible,  $\nu_{\text{AOH}} \ll 1$  (eq 8; see Scheme 1 for  $k_p$  and  $k_{\text{inh}}$  values).

$$\nu_{\text{TOH}} = \frac{k_p}{2k_{\text{inh}}} \frac{[\text{LH}]}{[\text{TOH}]} \quad (8)$$

The liposome solutions were injected into the wells of a microplate reader tray, and after equilibrating at 37 °C, azo free-radical initiator solutions were injected into the wells. We utilized as a source of peroxy radicals either 2,2'-azobis(2-amidinopropane) monohydrochloride (ABAP), a charged hydrophilic initiator with a half-life of  $579.4 \times 10^3$  s at 37 °C,<sup>22,47</sup> or 2,2'-azobis(4-methoxy-2,4-dimethyl valeronitrile) (MeO-AMVN), a lipophilic initiator with a half-life of  $12.8 \times 10^3$  s at 37 °C (Scheme 3).<sup>30</sup> Peroxyl radicals generated from ABAP are foreseen to react with the antioxidants at the water/membrane interface<sup>10</sup> approaching from the water,<sup>31</sup> whereas those from MeO-AMVN are expected to react approaching from the membrane hydrophobic core.<sup>30</sup> Values for  $R_g$  may be estimated from the thermolysis rate constant of the azo initiator  $k_i$  and the escape fraction of free radicals from geminate recombination  $e$  (eq 9 and Scheme 3).

$$R_g = 2ek_i[\text{azo initiator}] \quad (9)$$

### Scheme 3. Thermolysis of Azo Initiators<sup>22,30,47</sup>



Under the concentrations used ( $9 \times 10^{-3}$  M for ABAP,  $2 \times 10^{-4}$  M for MeO-AMVN), at 37 °C and under air-saturated conditions, peroxy radicals are generated at a constant rate  $R_g = 1 \times 10^{-8}$  M s<sup>-1</sup> in water<sup>22,23,47</sup> and toluene,<sup>30</sup> respectively. Geminate recombination (eq 10) has been shown to reduce by 11-fold the generation rate of lipophilic peroxy radicals from MeO-AMVN in lipid membranes, so the estimated value for  $R_g$  is  $\sim 0.91 \times 10^{-9}$  for MeO-AMVN in liposome solutions.<sup>30</sup>

Altogether, four antioxidant compounds were studied at six different concentrations in model membranes prepared from six different lipids in the presence of two types of peroxy radicals, in triplicates.

**Results Obtained with H<sub>2</sub>B-PMHC, EggPC, and ABAP.** Figure 2A displays representative intensity–time trajectories recorded in solutions containing ABAP, eggPC liposomes, and increasing concentrations of membrane-embedded H<sub>2</sub>B-PMHC. We recorded fluorescence intensity enhancements of  $\sim 100$ -fold, where the maximum emission intensity achieved was proportional to the initial concentration of the fluorogenic antioxidant used.

A linear increase in fluorescence intensity with time is observed following reaction of membrane-embedded H<sub>2</sub>B-PMHC with hydrophilic peroxy radicals. The linear increase in fluorescence intensity and concomitant linear drop in [H<sub>2</sub>B-PMHC] with time is consistent with the mechanism shown in Scheme 1, which predicts a rate law that is zero order for the consumption of a TOH antioxidant or analogue such as H<sub>2</sub>B-PMHC.<sup>23</sup> See also eqs 7 and 12, where  $\alpha$  is the proportionality constant between fluorescence intensity and [H<sub>2</sub>B-PMHC] and

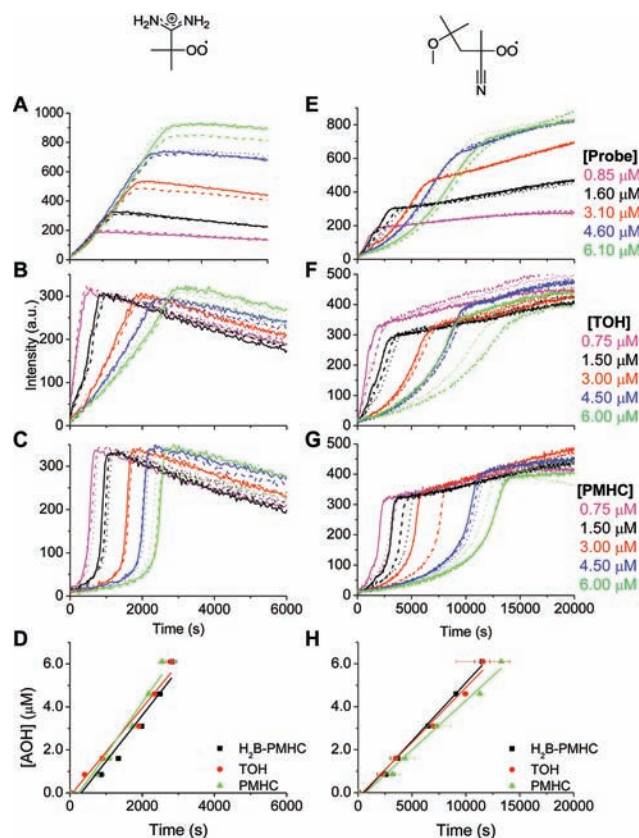


**Figure 2.** Fluorescence intensity–time profiles recorded in triplicates in 1 mM eggPC and  $9 \times 10^{-3}$  M ABAP solutions with increasing concentrations (see key to colors for the values) of (A) H<sub>2</sub>B-PMHC, (B) TOH + 0.1  $\mu\text{M}$  H<sub>2</sub>B-PMHC, and (C) PMHC + 0.1  $\mu\text{M}$  H<sub>2</sub>B-PMHC. (D) Increasing antioxidant concentration vs time required for its consumption ( $\tau$ ). Panels E–H show similar data acquired in 1 mM eggPC with  $2 \times 10^{-4}$  M MeO-AMVN.

is related to both the fluorescence detection efficiency of our setup and the emission quantum yield of oxidized H<sub>2</sub>B-PMHC.

$$\alpha \frac{d[\text{intensity}]}{dt} = -\frac{d[\text{H}_2\text{B-PMHC}]}{dt} = \frac{R_g}{2} \quad (12)$$

Figure 2B,C displays results obtained with increasing concentrations of membrane-embedded TOH or PMHC and a small, constant amount of H<sub>2</sub>B-PMHC as a signal carrier; otherwise the conditions were identical to those used in acquiring the data of Figure 2A. In both sets of data the maximum emission intensity achieved is the same in each run and proportional to the amount of H<sub>2</sub>B-PMHC used as signal carrier (note, however, that different microplate settings were used in acquiring data for Figure 2A versus panels B and C).

A linear increase in fluorescence intensity with time is observed for experiments conducted with TOH, with a slope that is inversely proportional to the initial [TOH] (Figure 2B). These results indicate that the peroxy radicals generated upon thermolysis of ABAP do not discriminate between the two antioxidants and react with the same rate constant with fluorogenic H<sub>2</sub>B-PMHC and with TOH; i.e.,  $k_{\text{inh}}^{\text{TOH}}/k_{\text{inh}}^{\text{H}_2\text{B-TOH}} \approx 1$  (see also below). The decreasing slope with increasing [TOH] simply indicates that, of the total antioxidant load (AOH, where  $[\text{AOH}]_0 = [\text{H}_2\text{B-PMHC}]_0 + [\text{TOH}]_0$ ) reacting at any given time, a decreasing fraction is fluorogenic. An induction period in the intensity profile is observed for

experiments with PMHC when ABAP is used (Figure 2C). These results highlight the higher reactivity (antioxidant activity) of membrane-embedded PMHC over H<sub>2</sub>B-PMHC toward hydrophilic peroxy radicals.

We conclude, on the basis of the observations listed above, that the reactivity order toward scavenging hydrophilic peroxy radicals at the water/membrane interface in eggPC liposomes is thus PMHC > TOH = H<sub>2</sub>B-PMHC.

**Results Obtained with H<sub>2</sub>B-PMHC, EggPC, and MeO-AMVN.** Qualitatively, the results obtained in experiments involving the generation of lipophilic peroxy radicals within eggPC liposomes followed the same trend as those described above using ABAP. Thus, a linear increase in fluorescence intensity with time was recorded for H<sub>2</sub>B-PMHC, the lipophilic peroxy radicals reacted with the same rate with TOH and H<sub>2</sub>B-PMHC, as reflected by a linear increase in intensity, and PMHC outcompeted H<sub>2</sub>B-PMHC, giving rise to induction periods (see Figure 2E–G). The major difference we encountered when comparing to experiments conducted with ABAP lies in the loss of linearity in the intensity plots occurring at smaller LH:H<sub>2</sub>BTOH molecular ratios (experiments conducted with  $4.6 \times 10^{-6}$  and  $6.1 \times 10^{-6}$  M total antioxidant load), which we assign to a larger time required for establishing steady-state conditions, given the small  $R_i$  value with MeO-AMVN, which is 10-fold smaller than that with ABAP under our experimental conditions due to free radical recombination within the membrane (eq 10).<sup>30</sup> Depletion of MeO-AMVN, which has a half-life of 12 800 s, may also contribute to the loss of linearity. Another important difference is that the shape of the induction period observed with PMHC is significantly less pronounced for lipophilic peroxy radicals than for hydrophilic peroxy radicals (Figure 2C vs G).

**Results Obtained with H<sub>2</sub>B-PMHC and All Other Lipids.** The outcome of experiments analogous to those described above, conducted on liposomes prepared with DLPC, DOPC, POPC, DMPC, or DPPC, are displayed in the Supporting Information, Figures S2–S6. The results obtained in these lipids with either hydrophilic or lipophilic peroxy radicals follow the same trend as those described above for eggPC liposomes.

In summary, from these qualitative observations, we conclude that the antioxidant activity toward either lipophilic or hydrophilic peroxy radicals follows the trend PMHC > TOH = H<sub>2</sub>B-PMHC. The three molecules differ solely in the structure of their lipophilic tails, yet they have the same inherent chemical reactivity given by their identical chromanol moiety. Our results highlight that both TOH and H<sub>2</sub>B-PMHC exhibit a restricted (yet similar) mobility and accessibility within the bilayer when compared to PMHC, a result of their large lipophilic tails. Differences in the antioxidant activities of these three compounds thus arise from membrane-induced changes in accessibility and mobility. In fact, all three molecules exhibit similar antioxidant activity in homogeneous solution, where competing kinetic studies show small yet identical induction periods with either PMHC or TOH (see Figure S7).

A quantitative treatment of the fluorescence intensity–time profiles is presented in the following section, wherefrom the relative antioxidant activities of PMHC, TOH, H<sub>2</sub>B-PMHC, and H<sub>2</sub>B-TOH are estimated for the various conditions.

**Results Obtained with H<sub>2</sub>B-TOH and Lipids.** Results from a series of experiments in which we monitored the fluorogenic antioxidant H<sub>2</sub>B-TOH in eggPC liposomes using either ABAP or MeO-AMVN azo initiators are displayed in Figure 3A–C

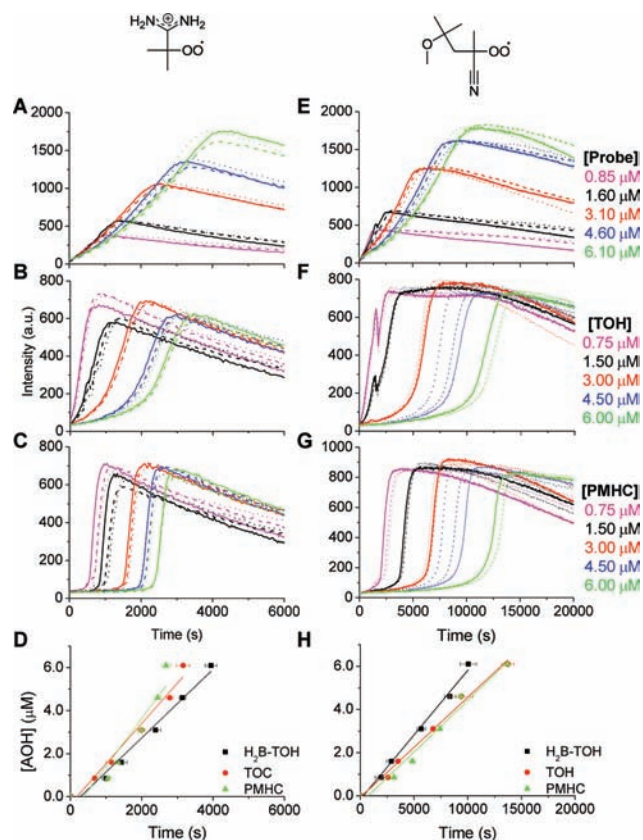


**Figure 3.** Fluorescence intensity–time profiles recorded in triplicates in 1 mM eggPC and  $9 \times 10^{-3}$  M ABAP solutions with increasing concentrations (see key to colors for the values) of (A) H<sub>2</sub>B-TOH, (B) TOH + 0.1 μM H<sub>2</sub>B-TOH, and (C) PMHC + 0.1 μM H<sub>2</sub>B-TOH. (D) Increasing antioxidant concentration vs time required for its consumption ( $\tau$ ). Panels E–H show similar data acquired in 1 mM eggPC with  $2 \times 10^{-4}$  M MeO-AMVN.

and E–G, respectively. Figures S9–S13 in the Supporting Information display the results gathered with DLPC, DOPC, POPC, DMPC, and DPPC. With H<sub>2</sub>B-TOH in the presence of peroxy radicals, we recorded fluorescence intensity enhancements of  $\sim 30$ -fold with time, where the maximum emission intensity achieved was proportional to the initial concentration of H<sub>2</sub>B-TOH employed.

A linear increase in intensity with time is observed following reaction of membrane-embedded H<sub>2</sub>B-TOH with peroxy radicals generated upon thermolysis of either ABAP or MeO-AMVN (Figure 3A,E). Notably, and as we described for experiments with H<sub>2</sub>B-PMHC above, deviations from linearity occur at small LH:H<sub>2</sub>B-TOH molecular ratios when lipophilic peroxy radicals are produced.

In all lipid suspensions examined, an induction period in the intensity profile is observed in experiments conducted with TOH and H<sub>2</sub>B-TOH as signal carrier and either ABAP or MeO-AMVN as source of peroxy radicals. The induction periods are significantly more pronounced in competitive kinetic studies with PMHC. These results highlight the higher reactivity of membrane-embedded TOH over H<sub>2</sub>B-TOH toward both hydrophilic and lipophilic peroxy radicals. They also show qualitatively that PMHC is more reactive than TOH. The reactivity order toward scavenging peroxy radicals is thus PMHC > TOH > H<sub>2</sub>B-TOH in all lipids examined with either lipophilic or hydrophilic peroxy radicals.

The lower reactivity toward peroxy radicals recorded for H<sub>2</sub>B-TOH over TOH may be ascribed to its lower inherent chemical reactivity (see also Figure S7 for homogeneous solution studies which show that  $k_{\text{inh}}^{\text{H}_2\text{B-TOH}}/k_{\text{inh}}^{\text{TOH}} \approx 0.25$ ).<sup>49</sup> The lower inherent reactivity of H<sub>2</sub>B-TOH arises from the electron-withdrawing effect of the carbonyl moiety in the ester linker functionality, which strengthens the phenol O–H bond.<sup>13</sup> Although the effect of a vicinal carbonyl on the antioxidant activity of a chromanol in homogeneous solution was established ~25 years ago, to our knowledge such an effect was not explored within lipid membranes. Here we show that the lipid membrane does not exert a leveling effect on antioxidant activities, and our results with H<sub>2</sub>B-TOH and TOH illustrate that even slight inherent chemical reactivity differences are translated to the heterogeneous water/lipid interface.

The higher reactivity of PMHC over TOH for peroxy radicals within lipid membranes has been described as arising from the higher accessibility and mobility of the former over the latter in these media. We show qualitatively that, whereas the induction periods recorded with hydrophilic peroxy radicals are more pronounced with PMHC than with TOH, for lipophilic peroxy radicals the induction curves are similar for both antioxidants. A more in-depth discussion is presented following the quantitative analysis below.

**Quantitative Analysis. Rates of Antioxidant Consumption.** The intensity–time trajectories recorded not only provide qualitative (*vide supra*) and quantitative (*vide infra*) information on the relative antioxidant activity of the four antioxidants studied but also enable us to calculate the rates of antioxidant consumption and the stoichiometric coefficient for peroxy radical scavenging by TOH and its analogues under the range of conditions explored. Alternatively, they may provide for an efficient way to determine rates of initiation of free radicals in a simple, rapid manner (see eqs 7 and 12).

The rates of antioxidant consumption may be calculated from the slope of the linear correlation between the concentration of total antioxidant load ( $[\text{AOH}]$ , where  $[\text{AOH}]_0 = [\text{fluorogenic antioxidant}]_0 + [\text{non-fluorogenic antioxidant}]_0$ ) and  $\tau$ , the time required for its consumption. Figure 2D,H illustrates the linear dependence of the initial antioxidant concentration  $[\text{AOH}]$  with  $\tau$  for experiments conducted in eggPC with H<sub>2</sub>B-PMHC and either ABAP or MeO-AMVN. Figure 3D,H illustrates similar data obtained in eggPC with H<sub>2</sub>B-TOH. Results with all other lipids are illustrated in Figures S1–S6 and S8–S13. Values of  $\tau$  were determined experimentally for each initial  $[\text{AOH}]$  from the intensity–time trajectories, such as those shown in Figures 2A–C, 2E–G, 3A–C, and 3E–G. The value of  $\tau$  corresponded to the time at the intercept of the straight lines tangential to the linear increase in intensity and the subsequent linear change in intensity arising from BODIPY degradation.<sup>40,41</sup>

The rates of antioxidant consumption we measured were roughly the same for all four antioxidants tested in all six lipids for a given type of azo initiator (either ABAP or MeO-AMVN), consistent with all four antioxidants having a stoichiometric coefficient of 2 for peroxy radical scavenging. The rates measured in the six different lipids are illustrated in the accompanying bar plots (Figure 4A,B for experiments with H<sub>2</sub>B-PMHC and Figure 4C,D for experiments with H<sub>2</sub>B-TOH); see also accompanying plots and Table S2 in the Supporting Information.

The rate values we measured with ABAP, in the range of  $1.5 \times 10^{-9}$ – $2.5 \times 10^{-9} \text{ M s}^{-1}$ , are 2- to 3-fold lower than the

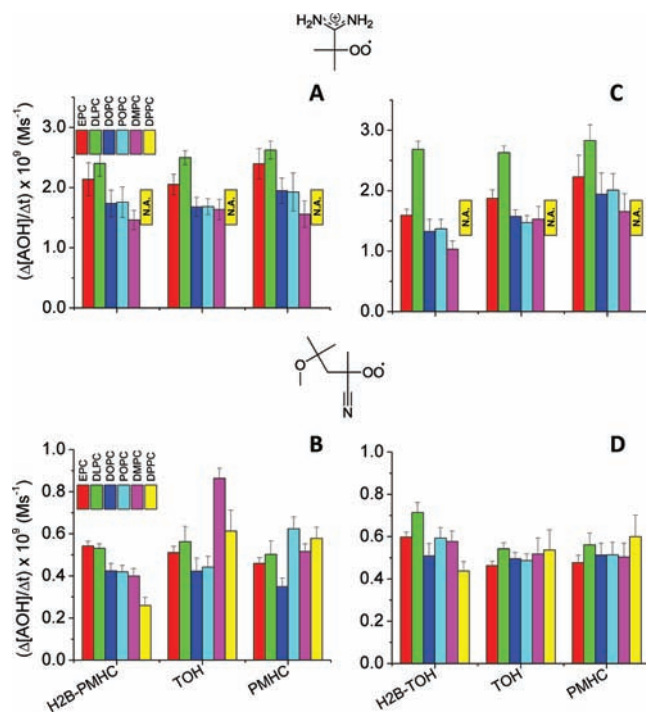


**Figure 4.** Rate of consumption of antioxidants determined in the presence of peroxy radicals in six different lipids. Panels A and B show the rates determined upon generation of peroxy radicals from  $9 \times 10^{-3} \text{ M}$  ABAP and  $2 \times 10^{-4} \text{ M}$  MeO-AMVN, respectively, acquired with the probe H<sub>2</sub>B-PMHC. Panels C and D show similar data acquired with the probe H<sub>2</sub>B-TOH.

theoretical estimate of  $5 \times 10^{-9} \text{ M s}^{-1}$  ( $R_g/2$ , see also eq 9 and accompanying discussion). Presumably a wastage reaction accounting for ~60% of the produced ROO<sup>•</sup> (and involving their bimolecular self-reaction) is taking place in the aqueous phase. Careful analysis of the bar plots shows that, with increasing unsaturation in the lipid utilized, the rate of hydrophilic peroxy radical consumption increases. Antioxidants embedded in saturated lipids do not efficiently scavenge hydrophilic peroxy radicals, presumably a result of their lower accessibility.

The rate values obtained with MeO-AMVN,  $0.5 \times 10^{-9}$ – $0.7 \times 10^{-9} \text{ M s}^{-1}$ , are ~10-fold lower than those expected in homogeneous solution with toluene as solvent ( $5 \times 10^{-9} \text{ M s}^{-1}$ ).<sup>30</sup> The discrepancy may be accounted for by geminate recombination within membranes (eq 10 in Scheme 3), which has been shown to reduce by 11-fold the generation rate  $R_g$  of lipophilic peroxy radicals from MeO-AMVN.<sup>30</sup> Lipophilic peroxy radicals are scavenged with the same efficiency by all four antioxidants studied, regardless of the nature of their aliphatic tail or the lipid membrane into which they are embedded.

In closing we also note that experiments in DMPC and DPPC are devoid of significant error, particularly when ABAP is used, possibly the result of a poor partitioning of the probe within saturated lipids. The low quality of the data prevents an accurate determination of the rate of consumption of AOH.

**Relative Antioxidant Activity.** The fluorescence intensity–time profiles may be further analyzed in order to determine the relative rate constants of H-atom abstraction for the various TOH analogues competing with the fluorogenic antioxidants.

The analysis of the rate law for the mechanism shown in Scheme 1, involving lipid autoxidation in the presence of a free-

**Scheme 4. Equations Employed in the Derivation of an Expression for Relative Antioxidant Activities Based on the Fluorescence Intensity-time Profiles for H<sub>2</sub>B-TOH**

$$-\frac{d[\text{TOH}]}{dt} = k_{\text{inh}}^{\text{TOH}} \left[ \frac{R_i}{2(k_{\text{inh}}^{\text{TOH}}[\text{TOH}] + k_{\text{inh}}^{\text{H}_2\text{B-TOH}}[\text{H}_2\text{B-TOH}])} \right] [\text{TOH}] \quad (13)$$

$$-\frac{d[\text{H}_2\text{B-TOH}]}{dt} = k_{\text{inh}}^{\text{H}_2\text{B-TOH}} \left[ \frac{R_i}{2(k_{\text{inh}}^{\text{TOH}}[\text{TOH}] + k_{\text{inh}}^{\text{H}_2\text{B-TOH}}[\text{H}_2\text{B-TOH}])} \right] [\text{H}_2\text{B-TOH}] \quad (14)$$

$$-\frac{d[\text{H}_2\text{B-TOH}]}{dt} = \frac{R_i}{2} \quad (15)$$

$$-\frac{d[\text{H}_2\text{B-TOH}]}{dt} = \left[ \frac{R_i}{2([\text{TOH}] + [\text{H}_2\text{B-TOH}])} \right] [\text{H}_2\text{B-TOH}] = \frac{R_i}{2} \frac{[\text{H}_2\text{B-TOH}]}{[\text{AOH}]} = \frac{R_i \beta}{2} \quad (16)$$

$$-\frac{d[\text{H}_2\text{B-TOH}]}{dt} = k_{\text{inh}}^{\text{H}_2\text{B-TOH}} \left[ \frac{R_i}{2k_{\text{inh}}^{\text{TOH}}[\text{TOH}]} \right] [\text{H}_2\text{B-TOH}] \quad (17)$$

$$-\frac{d[\text{H}_2\text{B-TOH}]}{dt} = k_{\text{inh}}^{\text{H}_2\text{B-TOH}} \left[ \frac{1}{k_{\text{inh}}^{\text{TOH}}(\tau - t)} \right] [\text{H}_2\text{B-TOH}] \quad (18)$$

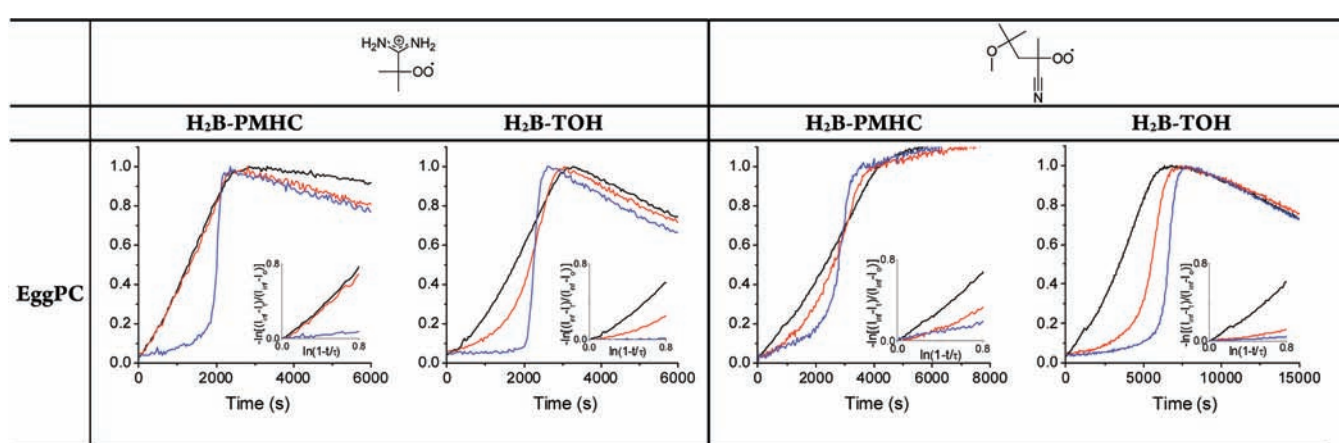


**Figure 5.** Fluorescence intensity–time traces acquired with ABAP and  $4.5 \times 10^{-6}$  M of either TOH or PMHC and  $0.1 \times 10^{-6}$  M of either H<sub>2</sub>B-TOH or H<sub>2</sub>B-PMHC in eggPC. Also shown are results acquired with MeO-AMVN as the source of peroxy radicals, with  $1.5 \times 10^{-6}$  M of either TOH or PMHC and  $0.1 \times 10^{-6}$  M H<sub>2</sub>B-PMHC, and with  $0.1 \times 10^{-6}$  M H<sub>2</sub>B-TOH and  $3.0 \times 10^{-6}$  M of either TOH or PMHC. The inset shows the analysis according to eq 20. Black, trajectories acquired with the probe alone; red, competitive kinetic experiments with the probe and TOH; and blue, competitive kinetic experiments with the probe and PMHC (in all cases the total load of antioxidant is the same).

radical initiator ROO<sup>•</sup> and TOH, and including a new antioxidant, e.g., H<sub>2</sub>B-TOH, shows that the rate of consumption of TOH may be described by eq 13 in Scheme 4. This equation is obtained upon substituting in eq 7 the expression for [LOO<sup>•</sup>] under steady-state conditions in the presence of two different antioxidants, e.g., H<sub>2</sub>B-TOH and TOH. A similar expression may be utilized to calculate the rate of consumption of H<sub>2</sub>B-TOH (or H<sub>2</sub>B-PMHC) in the presence of TOH (see eq 14). Based on the relative values of  $k_{\text{inh}}$ , three different regimes may be obtained for the rate of consumption of H<sub>2</sub>B-TOH:

(i) When  $k_{\text{inh}}^{\text{TOH}}[\text{TOH}] \ll k_{\text{inh}}^{\text{H}_2\text{B-TOH}}[\text{H}_2\text{B-TOH}]$ , the fluorogenic antioxidant consumption is unaffected by the presence of TOH (see eq 15).

(ii) When  $k_{\text{inh}}^{\text{TOH}}[\text{TOH}] = k_{\text{inh}}^{\text{H}_2\text{B-TOH}}[\text{H}_2\text{B-TOH}]$ , the rate of consumption of the fluorogenic antioxidant is reduced by the factor  $\beta$ , the ratio of fluorogenic antioxidant to total antioxidant (see eq 16).

(iii) When  $k_{\text{inh}}^{\text{TOH}}[\text{TOH}] \gg k_{\text{inh}}^{\text{H}_2\text{B-TOH}}[\text{H}_2\text{B-TOH}]$ , the differential equation obtained (see eq 17) may be solved by approximating  $[\text{TOH}]_t$  to the value obtained from the integral

of eq 7, where  $\tau$  is the time required for consuming the total  $[\text{TOH}]$  (see eq 18 in Scheme 4; a similar methodology is utilized in the analysis of the temporal evolution of oxygen uptake in the presence of antioxidants).<sup>10,13,20,47,50</sup>

Following integration, eq 19 is obtained, which may be further rearranged by replacing the ratio  $[\text{H}_2\text{B-TOH}]_t/[\text{H}_2\text{B-TOH}]_0$  in terms of the fluorescence intensities recorded in our experiment, to give eq 20, where  $I_0$ ,  $I_t$  and  $I_\infty$  are the initial intensity, the intensity at time  $t$ , and the intensity at the maximum.<sup>51</sup>

$$-\ln \left( \frac{[\text{H}_2\text{B-TOH}]_t}{[\text{H}_2\text{B-TOH}]_0} \right) = \frac{k_{\text{inh}}^{\text{H}_2\text{B-TOH}}}{k_{\text{inh}}^{\text{TOH}}} \ln \left( 1 - \frac{t}{\tau} \right) \quad (19)$$

$$-\ln \left( \frac{I_\infty - I_t}{I_\infty - I_0} \right) = \frac{k_{\text{inh}}^{\text{H}_2\text{B-TOH}}}{k_{\text{inh}}^{\text{TOH}}} \ln \left( 1 - \frac{t}{\tau} \right) \quad (20)$$

The above expression provides a simple way to determine the relative antioxidant activities for H<sub>2</sub>B-TOH and TOH ( $k_{\text{inh}}^{\text{H}_2\text{B-TOH}}/k_{\text{inh}}^{\text{TOH}}$ ) from the analysis of the initial slope of a plot of  $\ln[(I_\infty - I_t)/(I_\infty - I_0)]$  vs  $\ln(1 - t/\tau)$ . Such a protocol is

directly extendable to studies with PMHC or any other antioxidant. In an analogous manner, studies may be conducted with the more reactive fluorogenic antioxidant, H<sub>2</sub>B-PMHC. Equation 20 provides a more general way to evaluate the data than an analysis based on the initial slopes of intensity–time profiles.

Figures 5 and S14 show fluorescence intensity–time traces acquired with  $4.5 \times 10^{-6}$  M of either TOH or PMHC and  $0.1 \times 10^{-6}$  M of either H<sub>2</sub>B-TOH or H<sub>2</sub>B-PMHC, in all six lipids and with ABAP. Also shown are results acquired with MeO-AMVN as the source of peroxy radicals, in one case with  $1.5 \times 10^{-6}$  M of either TOH or PMHC and  $0.1 \times 10^{-6}$  M of H<sub>2</sub>B-PMHC, and in the second case with  $3.0 \times 10^{-6}$  M of either TOH or PMHC and  $0.1 \times 10^{-6}$  M of H<sub>2</sub>B-TOH. The insets show the intensity analysis according to eq 20 for trajectories both with probe alone and with probe and either TOH or PMHC. Note that, whereas the expected slope is 1 for trajectories acquired with the probe alone and analyzed according to eq 20, small deviations are observed when the actual fluorescence intensity enhancement is not linear with time.

Tables 1 and 2 list the relative antioxidant activities recorded in our studies in the presence of hydrophilic and lipophilic

**Table 1. Relative Antioxidant Activities in the Presence of Hydrophilic Peroxyl Radicals<sup>a</sup>**

lipid	$k_{\text{inh}}^{\text{H}_2\text{B-PMHC}}/k_{\text{inh}}^{\text{TOH}}$	$k_{\text{inh}}^{\text{H}_2\text{B-PMHC}}/k_{\text{inh}}^{\text{PMHC}}$	$k_{\text{inh}}^{\text{H}_2\text{B-TOH}}/k_{\text{inh}}^{\text{TOH}}$	$k_{\text{inh}}^{\text{H}_2\text{B-TOH}}/k_{\text{inh}}^{\text{PMHC}}$
eggPC	$0.94 \pm 0.02$	$0.10 \pm 0.01$	$0.39 \pm 0.02$	$\leq 0.01$
DLPC	$0.80 \pm 0.04$	$0.11 \pm 0.02$	$0.20 \pm 0.02$	$\leq 0.01$
DOPC	$0.96 \pm 0.03$	$0.11 \pm 0.01$	$0.31 \pm 0.02$	$\leq 0.01$
POPC	$1.10 \pm 0.01$	$0.13 \pm 0.02$	$0.37 \pm 0.02$	$\leq 0.01$
DMPC	$1.25 \pm 0.05$	$0.18 \pm 0.01$	$0.43 \pm 0.01$	$\leq 0.01$
DPPC	$1.17 \pm 0.1$	$0.10 \pm 0.02$	$0.56 \pm 0.01$	$\leq 0.01$

<sup>a</sup>The errors reported are those recovered from analyzing individual fluorescence intensity–time traces. Deviations from the average for three independent experiments are typically within 10%.

**Table 2. Relative Antioxidant Activities in the Presence of Lipophilic Peroxyl Radicals<sup>a</sup>**

lipid	$k_{\text{inh}}^{\text{H}_2\text{B-PMHC}}/k_{\text{inh}}^{\text{TOH}}$	$k_{\text{inh}}^{\text{H}_2\text{B-PMHC}}/k_{\text{inh}}^{\text{PMHC}}$	$k_{\text{inh}}^{\text{H}_2\text{B-TOH}}/k_{\text{inh}}^{\text{TOH}}$	$k_{\text{inh}}^{\text{H}_2\text{B-TOH}}/k_{\text{inh}}^{\text{PMHC}}$
eggPC	$0.57 \pm 0.03$	$0.18 \pm 0.02$	$0.17 \pm 0.01$	$0.06 \pm 0.01$
DLPC	$0.41 \pm 0.02$	$0.18 \pm 0.02$	$0.09 \pm 0.01$	$0.05 \pm 0.01$
DOPC	$0.52 \pm 0.02$	$0.13 \pm 0.03$	$0.12 \pm 0.01$	$0.05 \pm 0.01$
POPC	$0.75 \pm 0.02$	$0.14 \pm 0.02$	$0.19 \pm 0.01$	$0.05 \pm 0.01$
DMPC	$0.96 \pm 0.03$	$0.20 \pm 0.01$	$0.21 \pm 0.01$	$0.06 \pm 0.01$
DPPC	$0.96 \pm 0.02$	$0.30 \pm 0.02$	$0.21 \pm 0.02$	$0.01 \pm 0.01$

<sup>a</sup>The errors reported are those recovered from analyzing individual fluorescence intensity–time traces. Deviations from the average for three independent experiments are typically within 10%.

peroxyl radicals, respectively. A number of key new quantitative results are obtained upon inspection of the tabulated data:

(1) The relative antioxidant activities of chromanols in homogeneous solution, arising from their inherent chemical reactivity, readily translate to the microheterogeneous environment at the water/lipid interface; thus, similar values for  $k_{\text{inh}}^{\text{H}_2\text{B-PMHC}}/k_{\text{inh}}^{\text{H}_2\text{B-TOH}}$  (in the range of 2–3) are recorded in both homogeneous solution and liposome suspensions with hydrophilic or lipophilic peroxy radicals. Although the effect of a vicinal carbonyl on the antioxidant activity of a chromanol in

homogeneous solution was established ~25 years ago, to our knowledge such an effect was not explored within lipid membranes. Interestingly the lipid membrane does not exert a leveling effect on antioxidant activities, and our results with H<sub>2</sub>B-TOH and H<sub>2</sub>B-PMHC illustrate that even slight inherent chemical reactivity differences are translated to the heterogeneous water/lipid interface.

(2) The relative antioxidant activity between tocopherol analogues with the same inherent chemical reactivity but bearing short (PMHC) and long (TOH) aliphatic tails,  $k_{\text{inh}}^{\text{PMHC}}/k_{\text{inh}}^{\text{TOH}}$ , ranges from ~7 to ~9.4 (with the exception of DPPC, for which it is ~14) in the presence of hydrophilic peroxy radicals; on average, a value of 8 is found. Our results place in quantitative terms a long-known qualitative observation.<sup>8</sup>

(3) Lipophilic peroxy radicals show reduced discrimination between antioxidants bearing long and short aliphatic tails, with  $k_{\text{inh}}^{\text{PMHC}}/k_{\text{inh}}^{\text{TOH}}$  in the range of 3–5 when calculated from competing experiments performed with H<sub>2</sub>B-PMHC and in the range of 2–4 when calculated from competing experiments conducted with H<sub>2</sub>B-TOH for most lipid membranes. On average, the value lies between 3 and 4, based on either set of experiments. Notably,  $k_{\text{inh}}^{\text{PMHC}}/k_{\text{inh}}^{\text{TOH}}$  is lower for DLPC and exceptionally large for DPPC when acquired with H<sub>2</sub>B-TOH.

Points (2) and (3) constitute, to our knowledge, the first quantitative results on the relative antioxidant activity of TOH analogues bearing short vs long aliphatic tails. The higher reactivity of PMHC over TOH toward hydrophilic peroxy radicals has been ascribed to the higher accessibility to peroxy free radicals and higher mobility of the former over the latter in this media.<sup>8</sup> Our results show that accessibility to the antioxidant by the hydrophilic peroxy radical (a constraint imposed on hydrophilic but not lipophilic peroxy radicals) plays a significant role, yet the relative mobility of the peroxy radical and the antioxidant (a factor common to both types of peroxy radicals) is the dominant factor accounting for the difference between PMHC and TOH antioxidant activities in lipid membranes. We do, however, note that lipids are enriched with MeO-AMVN (a 2:10 MeO-AMVN/lipid mole ratio was used to ensure that peroxy radicals were generated at a sufficiently large rate), so the differences we observe between experiments conducted with hydrophilic vs lipophilic peroxy radicals may also arise from differences in the lipid membrane fluidity due to the inclusion of MeO-AMVN within the membranes.

Inspection of the traces in Figure 5 provides additional information, thus as described before:

(4) Antioxidants embedded in saturated lipids do not efficiently scavenge hydrophilic peroxy radicals, presumably a result of their lower accessibility, which translates in turn to longer times for antioxidant consumption. It may thus be observed, on going down the left two columns in Figure 5, that increasing times are required to consume the antioxidants as saturation in the lipids increases.

The above results add to a previous observation (vide supra), namely:

(5) Lipophilic peroxy radicals are scavenged with roughly the same efficiency by all four antioxidants studied, regardless of the nature of their aliphatic tail or the lipid membrane into which they are embedded.

A note of caution should be introduced to help rationalize the distribution of intensity–time traces around an average value for identical experimental conditions. Given the high activation energies for the thermolysis of AIBN (~130 kJ/mol)

or MeO-AMVN ( $\sim 115$  kJ/mol), these reactions are extremely sensitive to temperature. A change of 1 degree at 37 °C introduces changes of 15% and 13%, respectively, in the thermolysis rate constant  $k_i$  (see eq 9) of these azo initiators. A gradient of up to 1 °C across the wellplate was encountered in our experiments, and this affected the endpoint value (maximum intensity point) for triplicates. The relative antioxidant activity analysis based on eq 20, however, should not be affected significantly, provided the  $\tau$  value used is that recorded for each trajectory in, e.g., Figure 5.

## CONCLUSIONS

In conclusion, the two new fluorogenic TOH analogues reported here, characterized by different inherent chemical reactivity and large sensitivity, have enabled us to develop a high-throughput fluorescence method to study in real time the dynamics of antioxidant consumption in model lipid membranes. Our results illustrate that mobility and, to a lesser extent, physical accessibility account for the larger relative antioxidant activity of tocopherol analogues bearing short (PMHC) over long (TOH) aliphatic tails but that otherwise have the same inherent chemical reactivity. The results also illustrate that the microheterogeneous nature of the water/lipid interface does not exert a leveling effect on the antioxidant activities of TOH analogues that have different inherent chemicals reactivity toward H-atom abstraction.

The method we have developed is readily extendable to lipid mixtures including cholesterol and natural lipid mixtures. It should prove a powerful tool for oxidative lipidomics and, we argue, a range of analytical studies with the purpose of determining the extent of lipid degradation in, e.g., foods and oils. The new probes may be further utilized toward rapidly evaluating the rate of initiation of free radical reactions in complex systems with available fluorescence spectrometers. We also recognize the potential of the new probes toward imaging reactive oxygen species in live cell studies.

## EXPERIMENTAL SECTION

**Materials.** ( $\pm$ ) 6-Hydroxy-2,5,7,8-tetramethylchromane-2-carboxylic acid (Trolox),  $\alpha$ -tocopherol (TOH), 2,2,5,7,8-pentamethyl-6-chromanol (PMHC), diisopropyl azodicarboxylate, triphenylphosphine, and 2,2'-azobis-(2-methylpropionamide) dihydrochloride (ABAP) were purchased from Sigma-Aldrich (Oakville, Ontario, Canada). 2,2'-Azobis(4-methoxy-2,4-dimethylvaleronitrile) (MeO-AMVN) was supplied by Wako Pure Chemical Industries, Ltd. 1- $\alpha$ -Phosphocholine (eggPC), 1,2-dilinoleoyl-*sn*-glycero-3-phosphocholine (DLPC), 1,2-dioleoyl-*sn*-glycero-3-phosphocholine (DOPC), 1-palmitoyl-2-oleoyl-*sn*-glycero-3-phosphocholine (POPC), 1,2-dimyristoyl-*sn*-glycero-3-phosphocholine (DMPC), and 1,2-dipalmitoyl-*sn*-glycero-3-phosphocholine (DPPC) were obtained from Avanti Polar Lipids (Alabaster, AL). All chemicals were used without further purification. Water was purified by using a Millipore Milli-Q system.

**Methods.** Absorption and emission spectra were recorded on Cary 5000 UV-vis-NIR and Cary Eclipse fluorescence spectrophotometers, respectively, using 1 cm  $\times$  1 cm quartz cuvettes. H<sub>2</sub>B-TOH concentrations for wellplate assays were determined by measuring the absorption at  $\lambda_{\max} = 517$  nm in acetonitrile and using a molar absorption coefficient of 65 000 M<sup>-1</sup> cm<sup>-1</sup>. H<sub>2</sub>B-PMHC concentrations for wellplate assays were determined by measuring the absorption at  $\lambda_{\max} = 506$  nm in acetonitrile and using a molar absorption coefficient of 57 400 M<sup>-1</sup> cm<sup>-1</sup>. A Biotek Synergy 2 multi-mode microplate reader was used to record the intensity-time trajectories of the fluorogenic antioxidants H<sub>2</sub>B-TOH and H<sub>2</sub>B-PMHC. For experiments conducted with H<sub>2</sub>B-TOH, the fluorescence emission was recorded at 535 nm upon excitation at 490 nm. For

experiments conducted with H<sub>2</sub>B-PMHC, the fluorescence emission was recorded at 520 nm upon excitation at 485 nm. The emission was monitored for 14 h at 40 s time intervals. <sup>1</sup>H NMR and <sup>13</sup>C NMR spectra were recorded on a Varian VNMRS 500 instrument at 500 and 125 MHz, respectively. ESI mass spectra were measured on a Thermo Scientific Exactive Orbitrap.

**Liposome Preparation.** Aqueous solutions 20 mM in lipids were prepared as follows: 137 mg of eggPC, 141 mg of DLPC, 141 mg of DOPC, 137 mg of POPC, 122 mg of DMPC, and 132 mg of DPPC were weighed in six dry vials and dissolved with a minimal amount of chloroform. The solvent was evaporated with a stream of argon while rotating the sample vial to create a thin film on the vial wall. The films were left under vacuum to remove excess solvent. After 1 h the aliquots of eggPC, DLPC, DOPC, POPC, DMPC, and DPPC were hydrated with 9 mL of a pH 6.7, 10 mM PBS solution 150 mM in NaCl, yielding 20 mM lipid suspensions. The lipid suspensions were subjected to three freeze-thaw-sonication-vortex cycles, where each cycle involved storing the vials with the solutions in dry ice for 4 min and then thawing at 37 °C for 4 min, followed by 4 min sonication. After the third cycle, the lipid suspensions were extruded 15 times using an Avanti mini-extruder with one 100 nm polycarbonate membrane. Liposomes roughly 100 nm in diameter and each containing ca. 100 000 eggPC, DLPC, DOPC, POPC, DMPC, and DPPC lipids were thus obtained.<sup>1</sup>

**Microplate Assays. a. Increasing Concentration of H<sub>2</sub>B-TOH.** H<sub>2</sub>B-TOH was embedded in the lipid membranes as follows. A stock 130.7  $\mu$ M H<sub>2</sub>B-TOH solution in acetonitrile was prepared. H<sub>2</sub>B-TOH concentration was determined by measuring the absorption at  $\lambda_{\max} = 517$  nm in acetonitrile and using its molar extinction coefficient of 65 000 M<sup>-1</sup> cm<sup>-1</sup>. Five 64.3  $\mu$ L aliquots of 20 mM eggPC, DLPC, DOPC, POPC, DMPC, and DPPC (30 aliquots in total) were placed in microcentrifuge tubes and further diluted with 100  $\mu$ L of the PBS solution utilized in lipid hydration, to yield 7.8 mM lipid suspensions. To the five aliquots of a given lipid were added increasing amounts of H<sub>2</sub>B-TOH stock solution (8.4, 15.7, 30.5, 45.3, and 60  $\mu$ L, respectively). The solutions were subsequently diluted with the PBS solution, to yield 1.2 mL of solutions 1.07 mM in lipids and 0.91, 1.71, 3.32, 4.93, or 6.54  $\mu$ M in H<sub>2</sub>B-TOH. From each of the lipid suspensions, three aliquots of 280  $\mu$ L were loaded into three different wells of a microplate reader tray. The solutions were left equilibrating at 37 °C for 15 min, after which 20  $\mu$ L of free-radical initiator was added to each of the wells. The initiator solutions utilized were either 0.135 M in ABAP in a pH 6.7 PBS solution, or 3.0 mM in 2MeO-AMVN in acetonitrile. The final solutions were 1 mM in lipids, 10 nM in liposomes, 0.85, 1.6, 3.1, 4.6, or 6.1  $\mu$ M in H<sub>2</sub>B-TOH, and 9 mM in ABAP or 200  $\mu$ M in MeO-AMVN.

**b. Increasing Concentrations of PMHC or TOH with 0.1  $\mu$ M H<sub>2</sub>B-TOH.** PMHC or TOH and H<sub>2</sub>B-TOH were embedded in the lipid membranes as follows. Two antioxidant stock solutions were prepared containing (A) 12.9  $\mu$ M H<sub>2</sub>B-TOH in acetonitrile or (B) 128.6  $\mu$ M TOH or PMHC in acetonitrile. Lipid aliquots were prepared next as described above. To the five aliquots of a given lipid were added 10  $\mu$ L of stock solution A (H<sub>2</sub>B-TOH) and increasing amounts (7.5, 15, 30, 45, and 60  $\mu$ L respectively) of stock solution B (TOH or PMHC). The solutions were subsequently diluted with the PBS solution, to yield 1.2 mL of solutions of 1.07 mM in lipids, 0.107  $\mu$ M in H<sub>2</sub>B-TOH, and 0.8, 1.61, 3.21, 4.82, or 6.43  $\mu$ M in TOH or PMHC. The lipid suspensions were handled as described in the previous section for H<sub>2</sub>B-TOH only, including the addition of azo initiators. The final solutions were 1 mM in lipids, 10 nM in liposomes, 0.1  $\mu$ M in H<sub>2</sub>B-TOH, 0.75, 1.5, 3.0, 4.5, or 6.0  $\mu$ M in TOH or PMHC, and 9 mM in ABAP or 200  $\mu$ M in MeO-AMVN.

**c. Experiments with H<sub>2</sub>B-PMHC.** H<sub>2</sub>B-PMHC was embedded in the lipid membranes as described above for experiments conducted with H<sub>2</sub>B-TOH or H<sub>2</sub>B-TOH and TOH or PMHC. H<sub>2</sub>B-PMHC concentration was determined by measuring the absorption at  $\lambda_{\max} = 506$  nm in acetonitrile and using its molar extinction coefficient of 57 400 M<sup>-1</sup> cm<sup>-1</sup>. The procedure we followed was analogous to that described for H<sub>2</sub>B-TOH.

**Synthesis.** 8-Hydroxymethyl-1,3,5,7-tetramethyl pyrromethene fluoroborate was prepared as described in the literature.<sup>5</sup>

8-((±)-6-Hydroxy-2,5,7,8-tetramethylchroman-2-carbonyloxy)-methyl-1,3,5,7-tetramethylpyrromethene Fluoroborate (*H<sub>2</sub>B-TOH*). Trolox (0.1 g, 0.4 mmol, 1.5 equiv), 8-hydroxymethyl-1,3,5,7-tetramethylpyrromethene fluoroborate (0.074 g, 0.27 mmol, 1 equiv), and triphenylphosphine (0.105 g, 0.4 mmol, 1.5 equiv) were dissolved in 5 mL of dry THF under argon. The reaction mixture was left stirring for 5 min at 0 °C, and then diisopropyl azodicarboxylate (0.081 g, 0.4 mmol, 1.5 equiv) was added dropwise. After 10 min the ice bath was removed and the solution left to warm to room temperature. The reaction was left stirring at room temperature for 2 h. The solvent was evaporated under reduced pressure, and the residue was directly loaded onto a silica gel flash column and eluted with 1:1 hexane/dichloromethane in 1% methanol. The product was isolated as an orange powder (0.91 g, 67% yield): <sup>1</sup>H NMR (500 MHz, CDCl<sub>3</sub>) δ ppm 6.00 (s, 2H), 5.33 (d, *J* = 5.0 Hz, 1H), 5.11 (d, *J* = 4.7 Hz, 1H), 4.29 (s, 1H), 2.54–2.61 (m, 1H), 2.52, (s, 6H), 2.43–2.48 (m, 2H), 2.14 (s, 6H), 2.01 (s, 3H), 1.95 (s, 3H), 1.93 (s, 3H), 1.90–1.92 (m, 1H), 1.63 (s, 3H); <sup>13</sup>C NMR (125 MHz, CDCl<sub>3</sub>) δ ppm 173.9, 156.4, 145.9, 145.4, 141.4, 132.7, 132.3, 122.9, 122.1, 121.8, 118.9, 116.7, 57.7, 30.9, 25.6, 21.0, 15.3, 14.7, 12.1, 11.5, 11.0; HRMS (ESI<sup>+</sup>) for C<sub>28</sub>H<sub>33</sub>N<sub>2</sub>O<sub>4</sub>BF<sub>2</sub>Na (M<sup>+</sup>·Na) calcd 533.2394, found 533.2393; FTIR 3523, 1733, 1550, 1508, 1158, 975, 712 cm<sup>-1</sup>.

6-Methoxy-2,5,7,8-tetramethylchroman-2-carboxylate (**1a**). **1a** was prepared as described in the literature.<sup>52</sup> 6-Hydroxy-2,5,7,8-tetramethylchroman-2-carboxylic acid (Trolox, 1 g, 4 mmol) was dissolved in 10 mL of methanol, and dimethylsulfate (4.5 mL, 48 mmol) was added. Sodium hydroxide (2 g, 48 mmol) was dissolved in 10 mL of water and added dropwise to the solution. The reaction mixture was left stirring under argon at 70 °C for 2 days. The mixture was allowed to cool to room temperature and was poured into water, followed by extraction of the aqueous phase twice with dichloromethane and once with ethyl acetate. The organic extracts were washed with saturated aqueous NH<sub>4</sub>Cl solution and brine and were dried over MgSO<sub>4</sub>. After evaporation of the solvent under reduced pressure, the oily residue was loaded onto a silica gel flash column and eluted with 10% ethyl acetate/hexanes. Compound **1a** was obtained as oil (1.1 g, 98% yield): <sup>1</sup>H NMR (CDCl<sub>3</sub>, 500 MHz) δ ppm 3.70 (s, 3 H), 3.65 (s, 3 H), 2.64–2.64 (m, 1 H), 2.59–2.70 (m, 1 H), 2.40–2.57 (m, 2 H), 2.23 (s, 3 H), 2.20 (s, 3 H), 2.14 (s, 3 H), 1.82–1.94 (m, 1 H), 1.64 (s, 3 H); <sup>13</sup>C NMR (CDCl<sub>3</sub>, 126 MHz) δ ppm 174.2, 150.1, 147.7, 128.0, 125.6, 122.8, 117.1, 77.1, 60.3, 52.3, 30.5, 25.4, 20.9, 12.6, 11.8, 11.6; MS (ESI<sup>-</sup>) for C<sub>16</sub>H<sub>21</sub>O<sub>4</sub> (M<sup>-</sup>) calcd 277.15, found 277.13; FTIR 1751, 1753, 1453, 1250, 1102, 1080 cm<sup>-1</sup>.

6-Methoxy-2,5,7,8-tetramethylchroman-2-yl)methanol (**1b**). **1b** was prepared as described in the literature.<sup>53</sup> Lithium aluminum hydride (0.55 g, 14.4 mmol) was suspended in 15 mL of dry THF under argon at -78 °C. To the stirring suspension was added a solution of **1a** (1 g, 3.6 mmol) in 10 mL of dry THF dropwise. The reaction mixture was allowed to slowly warm to room temperature and was left stirring for 1 h. It was quenched by dropwise addition of water, followed by extraction with ethyl acetate. The organic fraction was washed with saturated aqueous NH<sub>4</sub>Cl solution and brine and dried over MgSO<sub>4</sub>, and the solvent was evaporated under reduced pressure. No further purification was required. Compound **1b** was obtained as a white solid (0.85 g, 95% yield): <sup>1</sup>H NMR (CDCl<sub>3</sub>, 500 MHz) δ ppm 3.55–3.72 (m, 5 H), 2.56–2.73 (m, 2 H), 2.21 (s, 3 H), 2.17 (s, 3 H), 2.07–2.13 (s, 3 H), 1.95–2.06 (m, 2 H), 1.75 (ddd, *J* = 13.5, 6.2, 4.8 Hz, 1 H), 1.25 (s, 3 H); <sup>13</sup>C NMR (CDCl<sub>3</sub>, 126 MHz) δ ppm 149.8, 147.1, 127.7, 126.2, 122.2, 117.2, 75.0, 69.4, 60.4, 27.5, 20.5, 20.1, 12.6, 11.9, 11.7; MS (ESI<sup>+</sup>) for C<sub>15</sub>H<sub>23</sub>O<sub>3</sub> (M<sup>+</sup>) calcd 251.16, found 251.09; FTIR 3260, 1451, 1245, 1043 cm<sup>-1</sup>.

6-Methoxy-2,5,7,8-tetramethylchroman-2-yl)methyl Trifluoromethanesulfonate (**1c**). **1c** was prepared as described in the literature.<sup>53</sup> **1b** (0.85 g, 3.4 mmol) was dissolved in 15 mL of dry dichloromethane under argon and cooled to 0 °C, and then pyridine (0.55 mL, 6.8 mmol) was added. Triflic anhydride (0.86 mL, 5.1 mmol) was added dropwise, and the reaction mixture was left stirring for 15 min at room temperature. The solution was then filtered

through silica gel to remove the excess Tf<sub>2</sub>O and triflic acid. The silica gel was further washed with 50% dichloromethane/hexanes. The filtrate was evaporated to dryness under reduced pressure to give compound **1c** as a white solid in quantitative yield (1.3 g): <sup>1</sup>H NMR (CDCl<sub>3</sub>, 500 MHz) δ ppm 4.48 (q, *J* = 1.0 Hz, 2 H), 3.65 (s, 3 H), 2.68 (t, *J* = 6.7 Hz, 2 H), 2.19–2.28 (m, 3 H), 2.17 (s, 3 H), 2.10 (s, 3 H), 1.95–2.05 (m, 1 H), 1.81–1.92 (m, 1 H), 1.38 (s, 3 H); <sup>13</sup>C NMR (CDCl<sub>3</sub>, 126 MHz) δ ppm 150.3, 146.3, 128.6, 125.9, 123.4, 122.5, 120.7, 119.9, 117.4, 116.6, 114.8, 79.6, 73.2, 72.9, 60.4, 60.4, 27.7, 21.0, 19.7, 12.5, 11.7; MS (ESI<sup>+</sup>) for C<sub>16</sub>H<sub>21</sub>F<sub>3</sub>O<sub>3</sub>S (M<sup>+</sup>) calcd 383.11, found 382.94; FTIR 1459, 1401, 1385, 1203, 1137 cm<sup>-1</sup>.

2-(6-Methoxy-2,5,7,8-tetramethylchroman-2-yl)acetonitrile (**1d**). **1c** (1.3 g, 3.4 mmol), 18-crown-6-ether (1.8 g, 6.8 mmol), and potassium cyanide (0.44 g, 6.8 mmol) were dissolved in 24 mL of dry acetonitrile at room temperature under argon. The reaction mixture was left stirring for 16 h and then diluted with ethyl acetate. The organic solution was washed twice with brine and dried over MgSO<sub>4</sub>, and the solvent was evaporated under reduced pressure. No further purification was required. Compound **1d** was obtained as an oil (0.86 g, 97% yield): <sup>1</sup>H NMR (CDCl<sub>3</sub>, 400 MHz) δ ppm 3.64 (s, 3 H), 2.55–2.74 (m, 4 H), 2.19 (s, 3 H), 2.15 (s, 3 H), 2.11 (s, 3 H), 1.87–2.07 (m, 2 H), 1.49 (s, 3 H); <sup>13</sup>C NMR (CDCl<sub>3</sub>, 101 MHz) δ ppm 150.3, 146.4, 128.6, 126.0, 123.5, 117.1, 116.5, 72.5, 60.4, 30.8, 28.5, 24.6, 20.3, 12.6, 11.8, 11.7; HRMS (ESI<sup>+</sup>) for C<sub>16</sub>H<sub>22</sub>O<sub>2</sub>N (M<sup>+</sup>) calcd 260.1645, found 260.1641; FTIR 2246, 1454, 1252, 1162, 1087 cm<sup>-1</sup>.

2-(6-Methoxy-2,5,7,8-tetramethylchroman-2-yl)acetic Acid (**2**). **1d** (0.86 g, 3.3 mmol) was dissolved in 5 mL of methanol. Potassium hydroxide (5.6 g, 100 mmol) was dissolved in 8 mL of water and added to the solution to yield a final concentration of 0.25 M **1d** and 7.7 M potassium hydroxide. The reaction mixture was stirring at 70 °C under argon for 24 h or until all the starting material was consumed. The solution was acidified with 6 M HCl and extracted with ethyl acetate. The organic extract was washed with brine and dried over MgSO<sub>4</sub>, and the solvent was evaporated under reduced pressure. The oily residue was loaded onto a short silica gel flash column and eluted with 50% ethyl acetate/hexanes. Compound **2** was obtained as white oily solid (0.57 g, 62% yield): <sup>1</sup>H NMR (CDCl<sub>3</sub>, 400 MHz) δ ppm 9.57–11.38 (bs, 1 H), 3.66 (s, 3 H), 2.69 (d, *J* = 4.7 Hz, 2 H), 2.65 (t, *J* = 6.8 Hz, 2 H), 2.21 (s, 4 H), 2.17 (s, 3 H), 2.03–2.14 (m, 5 H), 1.94 (dt, *J* = 13.8, 7.0 Hz, 1 H), 1.48 (s, 3 H); <sup>13</sup>C NMR (CDCl<sub>3</sub>, 101 MHz) δ ppm 176.4, 149.9, 146.8, 128.2, 125.9, 123.2, 117.2, 73.4, 60.4, 44.0, 31.0, 24.7, 20.5, 12.6, 11.8, 11.7; HRMS (ESI<sup>-</sup>) for C<sub>16</sub>H<sub>21</sub>O<sub>4</sub> (M<sup>-</sup>) calcd 277.1445, found 277.1441; FTIR 3500, 1701, 1447, 1252, 1084 cm<sup>-1</sup>.

8-((6-Hydroxy-2,5,7,8-tetramethylchroman-2-yl)-methyl)-1,3,5,7-tetramethyl Pyrromethene Fluoroborate (**3**), *H<sub>2</sub>B-PMHC*). **2** (0.17 g, 0.6 mmol) was dissolved in 0.7 mL of thionyl chloride and refluxed at 50 °C under argon for 1 h. The reaction mixture was diluted with 20 mL of dry toluene, and the solvent was evaporated to dryness under reduced pressure. The co-evaporation with toluene was repeated two more times, and the oily residue was dried under high vacuum for 2 h to ensure that all the thionyl chloride was removed. Without further purification, the oily residue was dissolved in 5 mL of dry dichloromethane. Phosphorus oxychloride (0.55 mL, 6 mmol) was added dropwise. The reaction mixture was stirred for 5 min at room temperature, followed by dropwise addition of 2,4-dimethylpyrrole (0.13 mL, 1.3 mmol). The reaction mixture was left stirring at room temperature under argon for 24 h. It was diluted with dichloromethane, washed with brine, and dried over MgSO<sub>4</sub>, and the solvent was evaporated under reduced pressure. The oily residue was redissolved in 5 mL of dry dichloromethane, and the solution was cooled to -10 °C. BBr<sub>3</sub> (0.55 mL, 6 mmol) was added dropwise, and the reaction mixture was stirred for 1 h at -10 °C. It was quenched with water and extracted with dichloromethane. The organic extract was washed with brine and dried over MgSO<sub>4</sub>, and the solvent was evaporated under reduced pressure. The oily residue was redissolved in 1 mL of dry dichloromethane and 12 mL of dry toluene. Diisopropylethylamine (0.4 mL) was added, followed after 15 min by very slow dropwise addition of BF<sub>3</sub>·OEt<sub>2</sub> (0.6 mL) at 0 °C. After stirring for 1.5 h at room temperature, the solvent was evaporated

under reduced pressure, and the residue was loaded onto a silica gel flash column and eluted with 30% ethyl acetate/hexanes. Compound **3** was obtained as red-orange solid (0.07 g, 23% yield over four steps):  $^1\text{H}$  NMR ( $\text{CDCl}_3$ , 500 MHz)  $\delta$  ppm 6.04 (s, 2 H), 4.20 (s, 1 H), 3.42–3.56 (m, 2 H), 2.57–2.74 (m, 2 H), 2.53 (s, 3 H), 2.52 (s, 3 H), 2.50 (s, 3 H), 2.43 (s, 3 H), 2.09 (s, 3 H), 2.08 (s, 3 H), 1.90–1.98 (m, 2 H), 1.77 (s, 3 H), 1.18;  $^{13}\text{C}$  NMR ( $\text{CDCl}_3$ , 126 MHz)  $\delta$  ppm 153.9, 153.1, 145.0, 144.7, 142.7, 141.2, 140.2, 134.6, 133.7, 123.3, 122.1, 122.0, 121.3, 118.3, 116.8, 75.6, 38.8, 33.4, 20.8, 17.6, 17.6, 14.5, 12.1, 11.5, 11.2; HRMS (ESI<sup>+</sup>) for  $\text{C}_{27}\text{H}_{34}\text{N}_2\text{O}_2\text{BF}_2$  ( $\text{M}^+$ ) calcd 467.2676, found 467.2683; FTIR 3547, 1543, 1194, 1152  $\text{cm}^{-1}$ .

## ■ ASSOCIATED CONTENT

### ■ Supporting Information

IR,  $^1\text{H}$  NMR, and  $^{13}\text{C}$  NMR of  $\text{H}_2\text{B-PMHC}$  and  $\text{H}_2\text{B-TOH}$ , and intensity–time trajectory plots for all conditions. This material is available free of charge via the Internet at <http://pubs.acs.org>.

## ■ AUTHOR INFORMATION

### Corresponding Author

gonzalo.cosa@mcgill.ca

### Notes

The authors declare no competing financial interest.

## ■ ACKNOWLEDGMENTS

G.C. is grateful to the Natural Sciences and Engineering Research Council (NSERC) and Canadian Foundation for Innovation (CFI) for funding. K.K. is thankful to the Drug Discovery and Training Program (CIHR) for postgraduate scholarships; S.F. is thankful to the NSERC USRA program for an undergraduate student research award. We are also grateful to Genevieve Redstone who conducted preliminary experiments with  $\text{H}_2\text{B-PMHC}$ .

## ■ REFERENCES

- (1) Burton, G. W.; Ingold, K. U. *Acc. Chem. Res.* **1986**, *19*, 194.
- (2) Singh, U.; Devaraj, S.; Jialal, I. *Annu. Rev. Nutr.* **2005**, *25*, 151.
- (3) Sano, M.; Ernesto, C.; Thomas, R. G.; Klauber, M. R.; Schafer, K.; Grundman, M.; Woodbury, P.; Growdon, J.; Cotman, C. W.; Pfeiffer, E.; Schneider, L. S.; Thal, L. J. *New Engl. J. Med.* **1997**, *336*, 1216.
- (4) Howard, A. C.; McNeil, A. K.; McNeil, P. L. *Nat. Commun.* **2011**, *2*, 597.
- (5) Boscoboinik, D.; Szewczyk, A.; Hensey, C.; Azzi, A. *J. Biol. Chem.* **1991**, *266*, 6188.
- (6) Azzi, A.; Gysin, R.; KempnÁ, P.; Munteanu, A.; Negis, Y.; Villacorta, L.; Visarius, T.; Zingg, J.-M. *Ann. N.Y. Acad. Sci.* **2004**, *1031*, 86.
- (7) Hasegawa, K.; Patterson, L. K. *Photochem. Photobiol.* **1978**, *28*, 817.
- (8) Niki, E.; Noguchi, N. *Acc. Chem. Res.* **2004**, *37*, 45.
- (9) Jonsson, M.; Lind, J.; Reitberger, T.; Eriksen, T. E.; Merenyi, G. *J. Phys. Chem.* **1993**, *97*, 8229.
- (10) Barclay, L. R. C. *Can. J. Chem.* **1993**, *71*, 1.
- (11) Liebler, D. C.; Baker, P. F.; Kaysen, K. L. *J. Am. Chem. Soc.* **1990**, *112*, 6995.
- (12) Liebler, D. C.; Burr, J. A.; Matsumoto, S.; Matsuo, M. *Chem. Res. Toxicol.* **1993**, *6*, 351.
- (13) Burton, G. W.; Doba, T.; Gabe, E.; Hughes, L.; Lee, F. L.; Prasad, L.; Ingold, K. U. *J. Am. Chem. Soc.* **1985**, *107*, 7053.
- (14) Barclay, L. R. C.; Edwards, C. E.; Vinqvist, M. R. *J. Am. Chem. Soc.* **1999**, *121*, 6226.
- (15) Barclay, L. R. C.; Vinqvist, M. R.; Mukai, K.; Itoh, S.; Morimoto, H. *J. Org. Chem.* **1993**, *58*, 7416.

(16) Roginsky, V.; Barsukova, T.; Loshadkin, D.; Pliss, E. *Chem. Phys. Lipids* **2003**, *125*, 49.

(17) Loshadkin, D.; Roginsky, V.; Pliss, E. *Int. J. Chem. Kinet.* **2002**, *34*, 162.

(18) Nam, T.-g.; Rector, C. L.; Kim, H.-y.; Sonnen, A. F. P.; Meyer, R.; Nau, W. M.; Atkinson, J.; Rintoul, J.; Pratt, D. A.; Porter, N. A. *J. Am. Chem. Soc.* **2007**, *129*, 10211.

(19) Valgimigli, L.; Ingold, K. U.; Lusztyk, J. *J. Am. Chem. Soc.* **1996**, *118*, 3545.

(20) Barclay, L. R. C.; Baskin, K. A.; Dakin, K. A.; Lock, S. J.; Vinqvist, M. R. *Can. J. Chem.* **1990**, *68*, 2258.

(21) Bowry, V. W.; Ingold, K. U. *Acc. Chem. Res.* **1999**, *32*, 27.

(22) Bedard, L.; Young, M. J.; Hall, D.; Paul, T.; Ingold, K. U. *J. Am. Chem. Soc.* **2001**, *123*, 12439.

(23) Alessi, M.; Paul, T.; Scaiano, J. C.; Ingold, K. U. *J. Am. Chem. Soc.* **2002**, *124*, 6957.

(24) Gramlich, G.; Zhang, J.; Nau, W. M. *J. Am. Chem. Soc.* **2004**, *126*, 5482.

(25) Barclay, L. R. C.; Vinqvist, M. R. *Free Radical Biol. Med.* **1994**, *16*, 779.

(26) Nam, T.-g.; Rector, C. L.; Kim, H.-y.; Sonnen, A. F. P.; Meyer, R.; Nau, W. M.; Atkinson, J.; Rintoul, J.; Pratt, D. A.; Porter, N. A. *J. Am. Chem. Soc.* **2007**, *129*, 10211.

(27) Sonnen, A. F. P.; Bakirci, H.; Netscher, T.; Nau, W. M. *J. Am. Chem. Soc.* **2005**, *127*, 15575.

(28) Culbertson, S. M.; Porter, N. A. *J. Am. Chem. Soc.* **2000**, *122*, 4032.

(29) Culbertson, S. M.; Vinqvist, M. R.; Barclay, L. R. C.; Porter, N. A. *J. Am. Chem. Soc.* **2001**, *123*, 8951.

(30) Noguchi, N.; Yamashita, H.; Gotoh, N.; Yamamoto, Y.; Numano, R.; Niki, E. *Free Radical Biol. Med.* **1998**, *24*, 259.

(31) Takahashi, M.; Tsuchiya, J.; Niki, E. *J. Am. Chem. Soc.* **1989**, *111*, 6350.

(32) Avila, D. V.; Ingold, K. U.; Lusztyk, J.; Green, W. H.; Procopio, D. R. *J. Am. Chem. Soc.* **1995**, *117*, 2929.

(33) Litwinienko, G.; Ingold, K. U. *Acc. Chem. Res.* **2007**, *40*, 222.

(34) Snelgrove, D. W.; Lusztyk, J.; Banks, J. T.; Mulder, P.; Ingold, K. U. *J. Am. Chem. Soc.* **2000**, *123*, 469.

(35) Wang, X.; Quinn, P. J. *Prog. Lipid Res.* **1999**, *38*, 309.

(36) Wang, X.; Quinn, P. J. *Mol. Membr. Biol.* **2000**, *17*, 143.

(37) Quinn, P. J. *Vitamin E: Vitamins and Hormones Advances in Research and Applications*; Elsevier: Amsterdam, 2007; Vol. 76, p 67.

(38) Atkinson, J.; Harroun, T.; Wassall, S. R.; Stillwell, W.; Katsaras, J. *Mol. Nutr. Food Res.* **2010**, *54*, 641.

(39) Qin, S.-S.; Yu, Z.-W.; Yu, Y.-X. *J. Phys. Chem. B* **2009**, *113*, 16537.

(40) Krumova, K.; Oleynik, P.; Karam, P.; Cosa, G. *J. Org. Chem.* **2009**, *74*, 3641.

(41) Oleynik, P.; Ishihara, Y.; Cosa, G. *J. Am. Chem. Soc.* **2007**, *129*, 1842.

(42) de Silva, A. P.; Gunaratne, H. Q. N.; Gunnlaugsson, T.; Huxley, A. J. M.; McCoy, C. P.; Rademacher, J. T.; Rice, T. E. *Chem. Rev.* **1997**, *97*, 1515.

(43) Khatchadourian, A.; Krumova, K.; Boridy, S.; Ngo, A. T.; Maysinger, D.; Cosa, G. *Biochemistry* **2009**, *48*, 5658.

(44) Krumova, K.; Cosa, G. *J. Am. Chem. Soc.* **2010**, *132*, 17560.

(45) *Liposomes*, 2nd ed.; Torchilin, V. P., Weissig, V., Eds.; Oxford University Press Inc.: New York, 2003; Vol. 264.

(46) Buttriss, J. L.; Diplock, A. T. *Biochim. Biophys. Acta (BBA)–Lipids Lipid Metab.* **1988**, *963*, 61.

(47) Barclay, L. R. C.; Locke, S. J.; MacNeil, J. M.; VanKessel, J.; Burton, G. W.; Ingold, K. U. *J. Am. Chem. Soc.* **1984**, *106*, 2479.

(48) Maillard, B.; Ingold, K. U.; Scaiano, J. C. *J. Am. Chem. Soc.* **1983**, *105*, 5095.

(49) We recently showed via oxygen uptake studies in styrene solution at 30 °C (ref 41) that TOH antioxidant activity towards peroxy radicals is ~1.6 fold larger than that of B-TOH, i.e.,  $k_{\text{inh}}^{\text{TOH}}/k_{\text{inh}}^{\text{B-TOH}} = 1.6$ . B-TOH bears ethyl groups in the BODIPY equatorial positions instead of H atoms as is the case for  $\text{H}_2\text{B-TOH}$ . The results

acquired with B-TOH are extendable to H<sub>2</sub>B-TOH since such structural modification only affects the photophysical properties of the probes yet it has no effect on their antioxidant activity.

(50) Barclay, L. R. C.; Ingold, K. U. *J. Am. Chem. Soc.* **1981**, *103*, 6478.

(51) Equation 20 requires for the experimental quantity observed to reach a plateau as the reaction is complete. In our experiments, and due to slow degradation of the probe once it is turned on as a result of further reaction between the peroxy radical and presumably the pyrrole units in the BODIPY, the intensity does not reach a plateau but rather decreases slowly. We thus use the intensity at the maximum as that corresponding to  $I_{\infty}$ .

(52) Koufaki, M.; Theodorou, E.; Galaris, D.; Nouis, L.; Katsanou, E. S.; Alexis, M. N. *J. Med. Chem.* **2005**, *49*, 300.

(53) Huang, J.-W.; Shiau, C.-W.; Yang, J.; Wang, D.-S.; Chiu, H.-C.; Chen, C.-Y.; Chen, C.-S. *J. Med. Chem.* **2006**, *49*, 4684.